

PACS numbers: 41.75.Fr; 52.80.–s; 42.55.Lt; 42.60.Lh
DOI: 10.1070/QE2010v040n07ABEH014335

Electron beam generation in open hollow-cathode discharge and the characteristics of He–Xe laser on the Xe line at $\lambda = 2.026$ μm

E.V. Bel'skaya, P.A. Bokhan, D.E. Zakrevskii

Abstract. **An open hollow-cathode discharge, generating an electron beam, is implemented in a cell with an active volume of 6.2 L. An electron-beam current of 3.4 A at an average power of 2.5 kW is obtained in helium in the quasi-cw regime at an anode voltage of 1.5 kV. Lasing in a He–Xe mixture on the $5d[3/2]_1^0 - 6p[3/2]_1$ transition in xenon at the wavelength $\lambda = 2.026$ μm under electron-beam excitation is investigated. The optimal component ratio in the He : Xe mixture is 99.5 : 0.5 ($p_{He} = 4–8$ Torr). The lasing power linearly increases with increasing the electron-beam power. It is shown that the discharge of this type can be used as an electron-beam source for exciting gaseous active media.**

Keywords: *electron beam, He–Xe laser, open discharge.*

1. Introduction

Electron beams (EBs) formed in vacuum diodes and electric discharges are used to excite active media of gas lasers. In the former case electrons are injected through separators into the laser active volume to be stopped and produce low-energy electrons. The drawbacks of this method are the necessity of using high-energy EBs (several hundreds of keV), difficulties related to the EB introduction into the active volume, and the need for high working-gas pressures. All these factors complicate laser design and limit the choice of the working medium because of an undesirable increase in the quenching rate of the upper active level under inelastic collisions.

Using the effect of electron runaway, one can form an EB directly in the laser active volume at working pressures of the active mixture. The runaway condition is implemented in discharges of different types, where emission is caused both by ions and fast atoms (high-voltage glow discharge, ultrahigh-density glow discharge, and Townsend discharge [1–3]) and by VUV radiation (open discharge [4, 5]). In [6] and some subsequent studies the possibility of pumping lasers by EBs formed in discharges of various designs and types was demonstrated [1, 7–10] and different light sources were designed [11, 12], including VUV sources [13]. Record lasing parameters per unit mass [14], as well as active region lengths [15, 16], were predicted and obtained for some active media.

E.V. Bel'skaya, P.A. Bokhan, D.E. Zakrevskii Rzhanov Institute of Semiconductor Physics, Siberian Branch, Russian Academy of Sciences, prosp. Akad. Lavrent'eva 13, 630090 Novosibirsk, Russia; e-mail: zakrdm@isp.nsc.ru

Received 2 April 2010; revision received 24 May 2010
Kvantovaya Elektronika **40** (7) 599–603 (2010)
Translated by Yu.P. Sin'kov

The main progress in laser pumping was made using nanosecond and submicrosecond EBs. Long (up to the cw regime) pulses either cannot be formed at all (for example, in barrier discharge [9]) or are difficult to obtain as a result of strong cathode sputtering [1, 17] or EB discharge instability in large volumes with a large cathode surface [4].

In this paper, we report the results of studying the possibility of generating high-power EBs in large-volume cells in long (up to the cw regime) pulses and demonstrate lasing in the test He–Xe medium on the xenon line at $\lambda = 2.026$ μm.

2. Experimental setup

A kind of open discharge – open hollow-cathode discharge [18–20] – was used to form a high-power continuous electron beam. The discharge is formed between a solid flat cathode and an anode, which are separated by a dielectric structure (DS) with holes. In EB discharges the anode location is generally of little importance [1]. In most cases it is located in the DS shadow. The beam emitted from the cathode passes through the DS and is stopped behind it in the drift space as a result of collisions with working gas atoms. As a result of EB stopping and electron multiplication in the residual field, ions drifting to the cathode are produced in DS channels. The space between the cathode and DS forms a cathode cavity, where the electric field is close to zero. The reason is that the DS inner surface is charged to a potential comparable with the cathode potential. As a result, the radial field distribution becomes significantly nonuniform both in the cavity and at the entrance of the DS holes [21]. Therefore, ions are concentrated at the hole's periphery. Having reached the region with a high potential gradient, these ions deviate from straight-line trajectories, enter the region with a small potential gradient, are slowed down due to elastic and inelastic collisions, and finally reach the cathode via ambipolar diffusion (which does not transport current). Due to this mechanism the ion current to the cathode is blocked, and electrons freely pass through the holes [21]. This allows one to obtain practical efficiency of EB generation (this parameter is defined as the ratio of the EB current to the discharge current) that exceeds 95% at energies of 1–5 keV. Such a high efficiency is provided by the photoemission caused by the resonant VUV irradiation of the working medium, excited upon slowing down of fast heavy particles in the cathode cavity [20, 21]. Specifically the mechanism of VUV generation radically differs the hollow-cathode discharge from the conventional open discharge, where VUV radiation is the result of excitation of working atoms by secondary electrons, and from other types of discharges generating EBs.

Previous studies of EB generation [18, 19] had a model character and were performed in a discharge chamber with a volume $V = 5$ cm^3 (the cathode area S did not exceed 2.5 cm^2).

We investigated the radial EB generation in a cylindrical chamber with cathode having a diameter $D = 8.4$ cm and length $L = 110$ cm ($V = 6200$ cm^3, $S = 2500$ cm^2). The chamber design is shown in Fig. 1. A voltage was applied between a stainless steel cathode (*1*) and coaxial electrodes, located at the cell end faces and playing the role of anode (*2*). Quartz rings (*3*) were fixed at a distance of 0.1 cm from the cathode using stainless steel bracings (*4*). The space between the cathode and quartz rings is the cathode cavity (*5*). The quartz rings had a width of 0.5 cm, a thickness of 0.35 cm, and an inner diameter (limiting the active region) of 7.6 cm; the distance between neighboring rings was 0.3 cm. Thus, the total cathode area was $S = 2500$ cm^2, and the area of its part unshielded by quartz rings was 1000 cm^2.

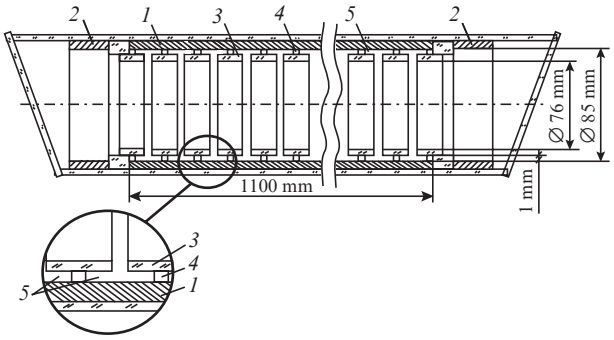

Figure 1. Schematic diagram of laser chamber: (*1*) cathode, (*2*) anode, (*3*) quartz ring, (*4*) metal ring, and (*5*) cathode cavity.

All experiments were performed after careful cell degassing by means of circulating helium, which was additionally purified using a liquid-nitrogen cooled activated carbon trap. Cell degassing and ageing were performed upon heating using both an external heater and a discharge in cw and quasi-cw regimes. All measurements were performed with circulation switched off, in the chamber filled with a gas under working pressure, at an average discharge power below the discharge power in the ageing regime.

The optical cavity was formed by two highly reflecting aluminium mirrors. Radiation was extracted from the cavity using a plane-parallel quartz plate. An InSb photodiode (PD24-03) with a maximum spectral sensitivity in the range of 1.95–2.1 μm and response time of 4 ns was used as photodetector; these parameters made it possible to investigate lasing on the xenon line at $\lambda = 2.026$ μm.

3. Study of EB generation

EB generation in helium was investigated in the cw and quasi-cw regimes with a pump-pulse repetition rate $f = 50$ Hz and voltage pulse FWHM $\tau = 10$ ms (half-period of line voltage). In the cw regime EB was formed when a voltage $U \geqslant 0.4$ kV was applied to the anode (the cathode was grounded). The beam generation was investigated with parameters varied in the following ranges: helium pressure $p_{He} = 2.6$–10 Torr, anode voltage $U = 0.4$–1.7 kV, current I up to 3.4 A, and the obtained current density $j = I/S = 1.36$ mA cm^{-2}. With an increase in the working voltage gas luminescence arises first in the ring near-wall region. The central part of the tube does not luminesce. The reason is that the EB formed is slowed down at a small distance from the wall because the working voltage is low and, correspondingly, the fast-electron path length is short. With an increase in voltage the luminescence gradually fills the entire cross section of the tube, and at $U \geqslant 1$ kV the radiation is concentrated (as in the conventional open discharge) closer to the tube centre [10].

The characteristics of discharge in He at different pressures are shown in Figs 2 and 3. Since the power introduced into the discharge volume is fairly high, the gas is heated, and its pressure grows with an increase in the power applied. Therefore, Figs 2 and 3 show the helium pressures assigned to room temperature; i.e., the pressures of the gas in a tube cooled to room temperature. Figure 2 shows the I–U characteristics of the discharge. When He pressure exceeds 5 Torr, a rather high power is introduced into the discharge volume, as a result of which the tube is heated. At $U < 1.3$ kV and $I < 1$ A the I–U characteristics were recorded in the cw regime, while at $U \geqslant 1.3$ kV and $I \geqslant 1$ A the measurements were performed in the quasi-cw regime ($f = 50$ Hz, voltage pulse FWHM 10 ms, current pulse FWHM ~8 ms).

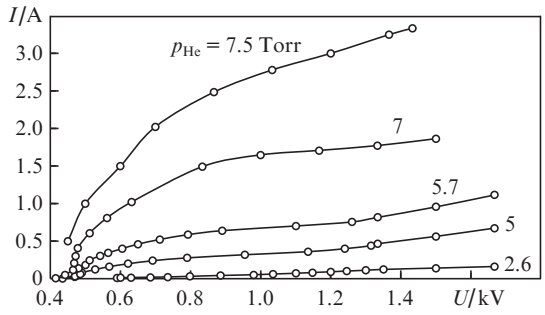

Figure 2. I–U characteristics of discharge at different helium pressures.

The dependence of current on He pressure at the same anode voltage amplitude $U = 1.5$ kV is shown in Fig. 3. An average EB power of 2.5 kW at a pulse power of 5 kW ($p_{He} = 7.5$ Torr, $U = 1.5$ kV, $I = 3.4$ A, $f = 50$ Hz) was reached in helium under quasi-cw excitation. At a dc voltage the dependence of the discharge current on helium pressure up to 5 Torr is described by the power law $I = 1.6\times10^{-2}p_{He}^{2.2}$ or $j = 6.4\times10^{-6}p_{He}^{2.2}$, where

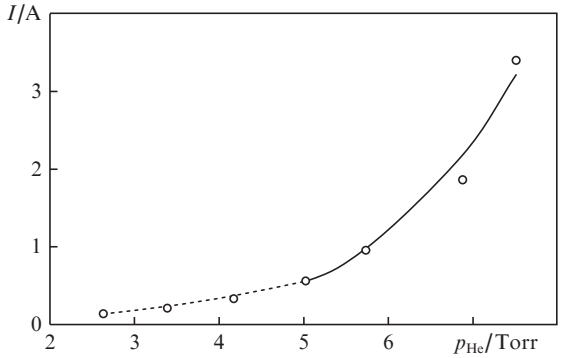

Figure 3. Dependence of the discharge current on helium pressure at $U = 1.5$ kV in the quasi-cw regime ($f = 50$ Hz, $\tau = 8$ ms): experimental data (circles), power-law function $I = 1.6\times10^{-2}p_{He}^{2.2}$ (dotted line), and $I = 4.5\times10^{-4}p_{He}^{4.4}$ (solid line).

the dimensions of current, pressure, and current density are, respectively, A, Torr, and A cm^{-2}. At $p_{He} > 5$ Torr the dependence $j(p_{He})$ changes as follows: $j = 1.8\times10^{-7}p_{He}^{4.4}$. Cw-regime discharges with photoemission [19, 21, 23] are characterised by a sharper dependence $j(p_{He})$ than the anomalous discharge: $j = 2.5\times10^{-12}p_{He}^{2}U^{3}$, where j is measured in A cm^{-2}, helium pressure is in torrs, and the voltage U is in volts [22].

The analysis of the cathode surface after the long-term (more than 300 h) cell operation during the generation of high-power EBs did not reveal any visible traces of its sputtering; this is an important practical feature of photoemission-sustained discharges. In the working-voltage range of 1–1.7 kV the EB generation efficiency, according to [18, 19, 21], exceeds 95% and only slightly depends on the characteristic hole size in the DS (distances between quartz rings) at the hole inner diameter $d \geqslant 3$ mm.

The EB generation in a He–Xe mixture was investigated in the pulsed regime ($f = 500$ Hz, voltage pulse width $\tau = 1.5$ s was limited by the characteristics of the power supply used) at helium and xenon pressures $p_{He} = 2$–10 Torr and $p_{Xe} = 3$–110 mTorr and anode voltage up to 2 kV (the cathode was grounded). The dependences of the discharge current on the partial pressures of the He–Xe mixture components are shown in Figs 4 and 5. An introduction of xenon changes the discharge parameters. At a constant voltage and helium pressure $p_{He} = 5$ Torr, an increase in the xenon pressure to $p_{Xe} = 50$ mTorr increases the current and, accordingly, the number of generated electrons in the He–Xe mixture by a factor of 2 (Fig. 4) in comparison with the current in helium under the same conditions but without xenon. In the range studied only at $p_{Xe} > 50$ mTorr the current ceases to depend on the xenon pressure. Introduction of xenon changes the amplitude of generated current, but the shape of the discharge I–U characteristic remains the same as for pure helium. Thus, the discharge current is determined by both the helium pressure (Fig. 3) and the xenon content in the mixture (Fig. 4). Figure 5 shows the dependences of the discharge current on helium pressure in the He–Xe mixture; these curves have extrema, in contrast to similar dependences for helium (Fig. 3). The maximum current is determined by only the ratio of component pressures in the He–Xe mixture and is independent of the anode voltage. In the range of $p_{He} = 2$–6 Torr at $p_{Xe} = 20$ mTorr the xenon content in the mixture is rather high; therefore, according to Fig. 4, the addition of xenon manifests itself only in the increase in current by a value that in the same for the entire range, and the increase in the current is on the whole due to the increase in p_{He}. At $p_{He} > 6$ Torr the increase in p_{He} and the change in the xenon content in the mixture (the factors determining the discharge current) act oppositely; however, the latter factor dominates, which explains the current drop in this range.

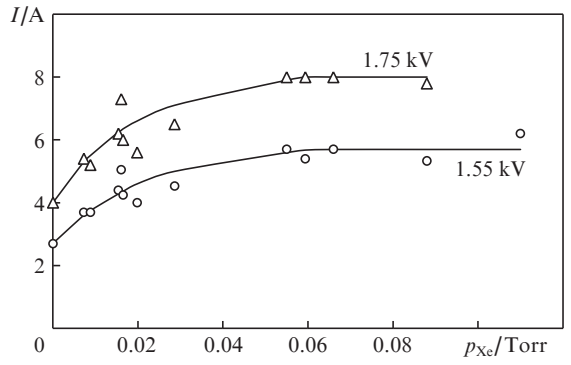

Figure 4. Dependences of the discharge current on xenon pressure in a He–Xe mixture at $U = 1.55$ and 1.75 kV and $p_{He} = 5$ Torr.

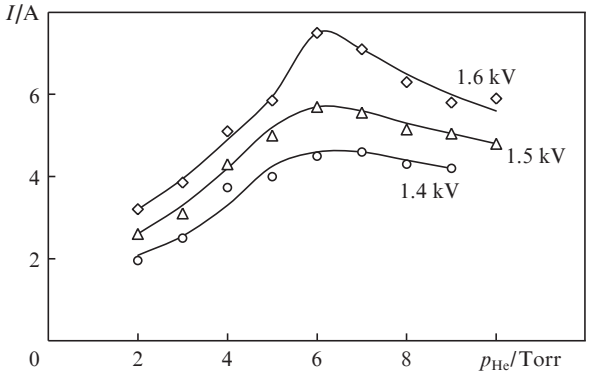

Figure 5. Dependences of the discharge current on helium pressure in a He–Xe mixture at $U = 1.4$, 1.5, and 1.6 kV and $p_{Xe} = 20$ mTorr.

4. Study of lasing in a He–Xe mixture

The experiments on excitation of He–Xe mixture were aimed at studying the possibility of lasing under gas pumping by electron beams obtained in open hollow-cathode discharge. This mixture was chosen as a convenient test medium, as in [6–9], where lasing in EB-pumped xenon was investigated.

We obtained and investigated lasing on the $5d[3/2]_1^0$–$6p[3/2]_1$ transition in xenon at $\lambda = 2.026$ μm. The lasing parameters were measured at $p_{He} = 2$–10 Torr, $p_{Xe} = 3$–110 mTorr, and anode voltage below 2 kV. The typical oscillograms of the anode voltage U, discharge current I, and lasing power P_{las} at $\lambda = 2.026$ μm in pulse are shown in Fig. 6. In the voltage and current oscillograms the first peak (0.75 μs wide) is due to the charge of spurious capacitance (~ 1 nF) of the laser supply circuit. The discharge current and voltage in the oscillograms

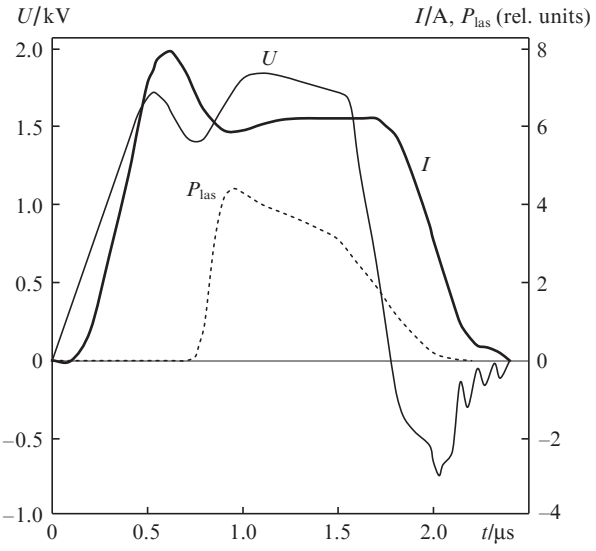

Figure 6. Typical oscillograms of anode voltage U, discharge current I, and lasing power at $p_{He} = 5$ Torr, $p_{Xe} = 0.025$ Torr, and $f = 500$ Hz.

are characterised by portions at $t > 0.75$ μs (counting from the beginning of the voltage pulse).

The dependences of the lasing power P_{las} and efficiency $\eta = P_{las}/P$ on the power $P = UI$ introduced into the discharge volume are shown in Fig. 7. The linear dependence $P_{las}(P)$ and the increase in η with P in the entire range under study indicate that the optimal EB current density, corresponding to the maximum radiation power, was not attained in the experiments. Correspondingly, at the pump powers under study, the electron mixing of xenon levels, which limits the growth of lasing power, does not occur. Therefore, one might expect the lasing efficiency to increase with a further increase in the discharge power and current.

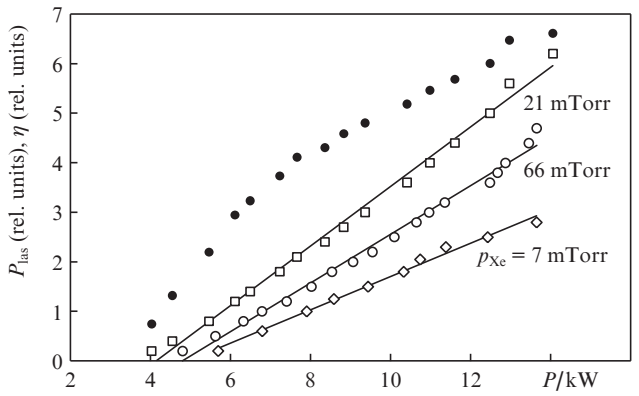

Figure 7. Dependences of the lasing power P_{las} (solid lines) and efficiency η (•) on the discharge power P in a He–Xe mixture at p_{Xe} = 7, 21, and 66 mTorr and p_{He} = 5 Torr.

The dependences $P_{las}(p_{He})$ and $I(p_{He})$ at p_{Xe} = 20 mTorr and different U are shown in Fig. 8. The lasing power depends on the EB current. Therefore, the pressure ratio in the mixture that is optimal for lasing on the xenon transition is determined by the pressure at which the discharge current is maximum (p_{Xe} = 20 mTorr and p_{He} = 6 Torr).

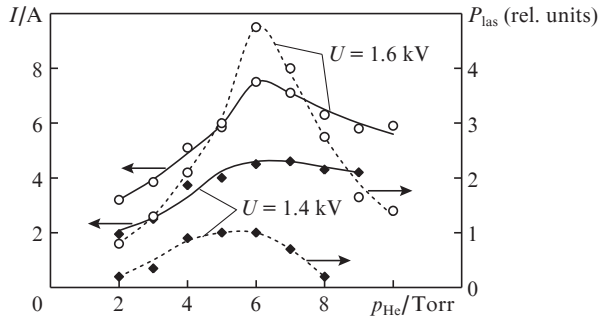

Figure 8. Dependences of the discharge current I and pulsed lasing power P_{las} on the helium pressure in a He–Xe mixture at U = 1.4 and 1.6 kV and p_{Xe} = 0.02 Torr.

The dependences of the lasing power on both xenon and helium pressures have extrema: at p_{He} = 5 Torr the optimal xenon pressure is in the range of 20–60 mTorr (Fig. 9). Specifically in this range the threshold discharge power P_{th}, at which lasing on the xenon line with λ = 2.026 μm arises, reaches a minimum (in the experiments the threshold power was determined as the discharge power at which P_{las} = 0.2 rel. units). With a decrease or increase in p_{Xe} the threshold voltage and current increase, and the lasing power decreases (provided that the discharge power remains the same). The concentration ratio He : Xe = 99.5 : 0.5 in the gas mixture is optimal for lasing.

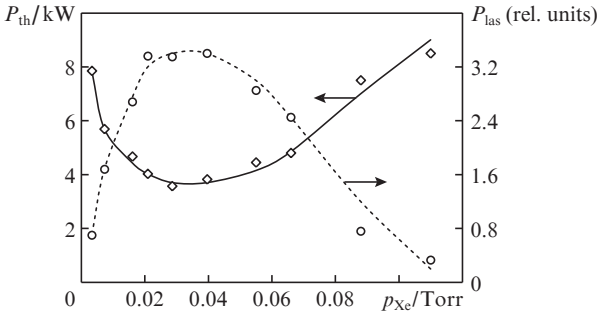

Figure 9. Dependences of the threshold discharge power P_{th} and lasing power P_{las} at P = 10 kW and p_{He} = 5 Torr.

Figure 10 shows the dependences of the pulsed (P_{las}) and average ($P_{las}^{av} = P_{las}f$) lasing power on the pump-pulse repetition rate. With a change in the repetition rate f from 100 to 1250 Hz the average lasing power increases by a factor of 14, reaching 95 mW. At the same time, the frequency dependence of the pulsed power P_{las} has an extremum: the sharp increase in the lasing power with an increase in frequency to f = 200 Hz changes with a gradual decrease at $f \geqslant 300$ Hz.

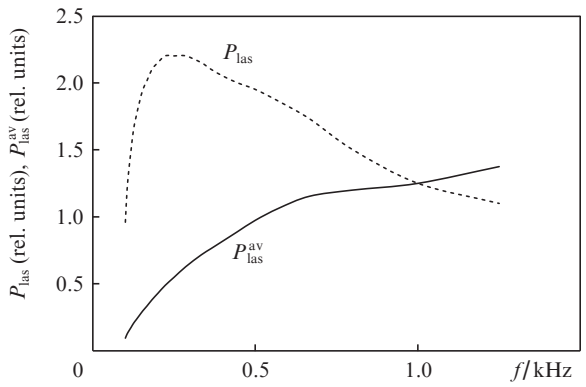

Figure 10. Dependences of the pulsed (P_{las}) and average (P_{las}^{av}) lasing powers on the pump-pulse repetition rate f.

5. Results and discussion

The main results of this study are as follows. It was experimentally shown that an open hollow-cathode discharge is stable in each cathode cavity, independently of their number and shape. Correspondingly, a significant increase in the cathode area (from S = 2.5 cm^2 in [18] to S = 2500 cm^2 in this study) and the use of slit cylindrical holes in the DS instead of rectangular or round ones does not lead to loss of discharge stability. The current density obtained in the cylindrical cell under study (D = 8.4 cm, L = 110 cm) is similar to that reported for the cell with a planar cathode diameter of 1.8 cm [18]. This fact is indicative of scalability of open hollow-cathode discharge.

It was shown in [18–21] that the EB generation efficiency exceeds 95% at $U > 1$ kV. These values should retain in our experiment, because the efficiency depends weakly on the area and geometry of the cathode open part and its characteristic size, exceeding 3 mm [21]. Based on the character of accelerating field in open discharges [21], one can suggest that the EB generated in discharge is monoenergetic, with the energy corresponding to the voltage applied. At a voltage $U > 1.5$ kV the EB energy is sufficient for crossing the cell aperture and exciting the entire cell volume; therefore, this beam can be used to pump laser media.

We obtained and investigated quasi-cw lasing on the transition in xenon at $\lambda = 2.026$ μm under EB excitation. The pulsed lasing power (with the same pump power) reaches a maximum at the concentration ratio He : Xe = 99.5 : 0.5 in the gas mixture ($p_{He} = 4–8$ Torr) (Fig. 9), when the threshold power is minimum. This ratio is also optimal for dense gases, at buffer gas pressures of 1–3 atm [24]. The dependence of the lasing power on the discharge power in the ranges of parameters under study is linear at a voltage U below 2 kV and discharge current below 10 A. Under the optimal conditions the highest obtained pulsed lasing power exceeds 100 W, with a practical efficiency above 1%. Apparently, application of a higher-Q cavity will make it possible to increase both pulsed and average lasing powers.

6. Conclusions

An open hollow-cathode discharge, stably generating an electron beam, was implemented in a large coaxial cell ($V = 6.2$ l, $D = 8.5$ cm, $L = 110$ cm). An average EB power of 2.5 kW at an anode voltage of 1.5 kV and helium pressure of 7.5 Torr was obtained in the quasi-cw regime in helium; this power is sufficient for exciting the entire volume of laser cell. Lasing was realised on the $5d[3/2]^0_1 – 6p[3/2]_1$ atomic transition in xenon at $\lambda = 2.026$ μm under excitation of He–Xe mixture by an EB generated in open hollow-cathode discharge.

The results obtained indicate that open hollow-cathode discharge can be used as a source of electron beam for exciting gas lasers. In our opinion, this type of pumping is most promising for ion metal vapor lasers (He–Cd, He–Zn, etc.) [25].

References

1. Rocca J.J., Meyer J.D., Farrell M.R., Collins G.J. *J. Appl. Phys.*, **56**, 790 (1984).
2. Hartmann P., Matsuo H., Ohtsuka Y., et al. *Jpn. J. Appl. Phys.*, **42**, 3633 (2003).
3. Ul'yanov K.N. *Teplofiz. Vys. Temp.*, **43**, 645 (2005).
4. Bokhan P.A., Sorokin A.R. *Zh. Tekh. Fiz.*, **55**, 88 (1985).
5. Bokhan P.A. *Entsiklopediya nizkotemperaturnoi plazmy* (Encyclopedia of Low-Temperature Plasma). Ed. by Fortov V.E. (Moscow: Fizmatlit, 2005) Ser. B, Vol. XI-4, p. 316.
6. Bokhan P.A., Sorokin A.R. *Pis'ma Zh. Tekh. Fiz.*, **8**, 947 (1982).
7. Kolbychev G.V., Samyshkin E.A. *Kvantovaya Elektron.*, **10**, 437 (1983) [*Sov. J. Quantum Electron.*, **13**, 249 (1983)].
8. Bokhan P.A., Sorokin A.R. *Opt. Quantum Electron.*, **23**, 523 (1991).
9. Azarov A.V., Mit'ko S.V., Ochkin V.N. *Kvantovaya Elektron.*, **32**, 675 (2002) [*Quantum Electron.*, **32**, 675 (2002)].
10. Bel'skaya E.V., Bokhan P.A., Zakrevsky D.E. *Kvantovaya Elektron.*, **38**, 823 (2008) [*Quantum Electron.*, **38**, 823 (2008)].
11. Muratov E.A., Rakhimov A.T., Suetin N.V. *Zh. Tekh. Fiz.*, **74** (5), 121 (2004).
12. Ashurbekov N.A., Iminov K.O., Kobzeva V.S., et al. *Izv. Vyssh. Uchebn. Zaved., Ser. Fiz.*, **4**, 89 (2009).
13. Jiang Ch., Kuthi A., Gundersen M.A., Hartmann W. *Appl. Phys. Lett.*, **87**, 131501 (2005).
14. Bokhan P.A. *Pis'ma Zh. Tekh. Fiz.*, **12**, 161 (1986).
15. Arlantsev S.V., Borovich B.L., Buchanov V.V. *J. Russ. Laser Research*, **16**, 99 (1995).
16. Bokhan P.A., Molodykh E.I., in *Pulsed Metal Vapour Lasers* (Dordrecht–Boston–London: Kluwer Acad. Press, 1996) p. 137.
17. Jánossy M., Rózsa K., Csillag L., Bergou J. *Phys. Lett. A*, **68** (3-4), 317 (1978).
18. Bokhan P.A., Zakrevsky D.E. *Appl. Phys. Lett.*, **81**, 2526 (2002).
19. Bokhan P.A., Zakrevsky D.E. *Pis'ma Zh. Tekh. Fiz.*, **28** (2), 74 (2002).
20. Bokhan P.A., Zakrevsky D.E. *Pis'ma Zh. Tekh. Fiz.*, **28** (11), 21 (2002).
21. Bokhan P.A., Zakrevsky D.E. *Fiz. Plazmy*, **32**, 853 (2006).
22. Klimenko K.A., Korolev Yu.D. *Zh. Tekh. Fiz.*, **60** (9), 138 (1990).
23. Belskaya E.V., Bokhan P.A., Zakrevsky D.E. *Appl. Phys. Lett.*, **93**, 091503 (2008).
24. Sereda O.V., Tarasenko V.F., Fedenev A.V., Yakovlenko S.I. *Kvantovaya Elektron.*, **20**, 535 (1993) [*Quantum Electron.*, **23**, 515 (1993)].
25. Ivanov I.G., Latush E.L., Sem M.F. *Ionnye lazery na parakh metallov* (Ion Metal Vapor Lasers) (Energoatomizdat: Moscow, 1990).